Ab initio description of monovacancies in paramagnetic austenitic Fe-Cr-Ni alloys

L. Delczeg,[1] B. Johansson,[1,2] and L. Vitos[1,2,3]

[1]*Applied Materials Physics, Department of Materials Science and Engineering, Royal Institute of Technology, SE-10044 Stockholm, Sweden*
[2]*Division for Materials Theory, Department of Physics and Materials Science, Uppsala University, Box 516, SE-75120 Uppsala, Sweden*
[3]*Research Institute for Solid State Physics and Optics, H-1525 Budapest, P.O. Box 49, Hungary*

(Received 13 December 2011; revised manuscript received 1 March 2012; published 1 May 2012)

Using first-principles alloy theory, we calculate the vacancy formation energies of paramagnetic face-centered-cubic (fcc) Fe-Cr-Ni alloys as a function of chemical composition. These alloys are well-known model systems for low carbon austenitic stainless steels. The theoretical predictions obtained for homogeneous chemistry and relaxed nearest-neighbor lattice sites are in line with the experimental observations. In particular, Ni is found to decrease and Cr to increase the vacancy formation energy of the ternary system. The results are interpreted in terms of effective chemical potentials. The impact of vacancy on the local magnetic properties of austenitic steel alloys is also investigated.

DOI: 10.1103/PhysRevB.85.174101 PACS number(s): 61.72.jd, 71.15.Nc, 71.20.Be, 81.05.Bx

I. INTRODUCTION

One of the most important steps in the history of humanity which accelerated the development of the modern industry and technical world was the discovery of steels. After successful integration within most of the common technologies the increasing scientific interest for studying the fundamental properties of steel is quite natural. Major attention is placed on different tests of various steels to select the best grades to be used under extreme conditions, found for example in nuclear power plants. Vacancies are well-known defects at high temperature and also in irradiated materials.[1–5] Today reliable experimental data for the formation energy of monovacancies exist for most of the metals and a large number of alloys.

The theoretical description of the formation energy of monovacancies has always been a benchmark for the theoretical approaches like the exchange-correlation approximations in density functional theory.[6] This is because vacancies involve both slowly and rapidly varying density regimes. The prior corresponds to the oscillating metallic density around the vacancy and the latter to the electronic surface near the core of the vacancy. Despite of obvious similarities, vacancies scan a rather different range of the inhomogeneous electronic density compared to metal surfaces[7] and thus require a special approach. The local-density approximation (LDA)[8] describes accurately the nearly homogeneous electron gas, e.g., regions far from the vacancy core, but is expected to break down in systems with rapid density variations. To incorporate effects due to inhomogeneous electron density, researchers made use of the density gradient expansion of the exchange-correlation functional[8] and arrived at the so-called generalized gradient approximation (GGA). Nowadays, the most commonly accepted and used GGA is the Perdew-Burke-Ehrzenhoff (PBE) functional proposed by Perdew *et al.*[9]

A number of theoretical studies focused on the *ab initio* determination of the formation energies and crystal structure of vacancies in metals.[10–17] Most of these investigations employed density functional theory based on LDA or on gradient-level approximations from the aforementioned functional family.

In the present work, our aim is to calculate the monovacancy formation enthalpy for the paramagnetic face-centered-cubic (fcc) Fe-Cr-Ni alloy. The commercial AISI 302, 304, and 316 grades are well-known low carbon austenitic stainless steels, in which the Fe-Cr-Ni alloy forms about 95 weight percent (wt. %) of the total composition. In these alloys, the Ni content varies from 8 to 14 wt. %, while the Cr content varies from 17 to 20 wt. %, whereas the carbon content is kept under 0.08 wt. %. Other important substitutional alloying elements are Si, Mn, and, respectively, Mo for some AISI 316 alloys. These elements are added to control carbon solubility and improve the heat resistant properties.[1] It was reported that in Fe-based alloys containing 0.08 wt. % C, 18 wt. % Cr, and 14 wt. % Ni alloy the interaction between carbon and vacancy is negligible.[18] Hence our paramagnetic fcc Fe-Cr-Ni alloy is expected to be a reasonable model system for the realistic austenitic stainless steels, from the point of view of the vacancy formation energy. Although the other minor alloy components can also interact with the monovacancies, in the present study we omit them and focus on the vacancy formation energy in homogeneous paramagnetic fcc Fe-Cr-Ni ternary system. Using a paramagnetic random solid solution model means that we neglect the direct description of the interaction between the major elements (Fe, Cr, and Ni) and the vacancy, and also the influence of the vacancy on the magnetic state. Nevertheless, as we will see, the good correspondence between the present theoretical and the available experimental data confirms the above approximations. Furthermore, the disclosed composition dependence of the vacancy formation energy can be used to derive useful information about the solute-vacancy interaction in the present ternary alloy.

The structure of the paper is the following. The theoretical tool is presented in Sec. II, where we also give the most important details of the numerical calculations. The results are presented in Sec. III. Here, we start by establishing the accuracy of the present computational method by making use of the former theoretical data. In Sec. IV, we compare our results to the available experimental data and finally we discuss the alloying effects on the formation energy and the impact of the vacancy on the bulk properties.

II. COMPUTATIONAL METHOD

A. Total-energy calculations

All calculations have been carried out using density functional theory[6,8] formulated within the exact muffin-tin orbital (EMTO) method[19–22] in combinations with supercell technique[17] and the mean-field coherent-potential approximation (CPA).[23] The EMTO method is similar to the screened Korringa-Kohn-Rostoker method, where the one-electron potential is represented by large overlapping muffin-tin potential spheres. By using overlapping spheres, one describes more accurately the crystal potential, when compared to the conventional nonoverlapping muffin-tin approach.[22,24] The EMTO method, in combination with the full charge density technique,[25] has been applied successfully in the theoretical study of the thermophysical properties of metallic alloys.[21,22,26–36]

In the self-consistent calculations, the exchange-correlation term was described within the local-density approximation. Here we adopted the Perdew and Wang parametrization[37] of the quantum Monte Carlo data by Ceperley and Alder.[38] The total energy and thus the vacancy formation energy was obtained within the PBE approximation. PBE approximation gives a rather accurate equilibrium volume for the Fe-Cr-Ni alloys,[39] which is essential for the proper account of the magnetic state.[40] The PBE gradient term in the total energy was included within the perturbative approach.[41] Namely, we used the total charge density obtained within LDA to compute the gradient-level total energies. This approach suits very well the full charge density formalism[25] and has been shown to produce errors which are within the numerical accuracy of our calculations.[42,43]

At ambient conditions, the Fe-Cr-Ni alloys have the fcc crystallographic structure of γ-Fe and are paramagnetic. The substitutional disorder on the fcc underlying lattice was treated within the CPA. This approach neglects the effect of local lattice relaxation and short-range order. However, as demonstrated by several former applications, the EMTO-CPA scheme yields rather accurate total energies for Fe-Cr-Ni alloys.[17,27–29] The paramagnetic state was modeled using the disordered local magnetic moment (DLM) approach[29,44–46] in combination with the CPA. According to that, the ternary $Fe_{1-c-n}Cr_cNi_n$ alloy is treated as a four-component $Fe^{\uparrow}_{(1-c-n)/2}Fe^{\downarrow}_{(1-c-n)/2}Cr_cNi_n$ system, with equal amount of spin-up and spin-down components. Note that within the DLM picture, no local magnetic moments develop on Cr and Ni atoms.

B. Vacancy formation energy

We started our investigation by establishing the equation of state of Fe-Cr-Ni. For each chemical composition, the bulk total energy was calculated for nine different volumes around the expected equilibrium volume. The theoretical equilibrium Wigner-Seitz radius (w_0), bulk total energy (E_0), and bulk modulus (B_0) were extracted from a Morse type of function[47] fitted to the calculated total energies.

For the vacancy formation energy, we used supercells built up from the conventional fcc unit cell. Previously, the effect of the size of the supercell on the vacancy formation energy was thoroughly examined for several fcc metals.[11,17,21] It was found that, as long as the proper convergence of the Brillouin-zone sampling is ensured, relatively small supercells are already enough for an accurate description of the vacancy formation energies. Because of that, here we adopted a $2 \times 2 \times 2$ supercell with simple cubic (sc) symmetry and with 32 sites per primitive cell. One of the 32 sites was substituted by a vacancy corresponding to $1/32$ vacancy concentration in the homogeneous bulk alloy.

To obtain the unrelaxed vacancy formation energy (H_{fu}), first we calculated the equilibrium Wigner-Seitz radius ($w_{\rm SC}$) and the total energy [$E_{\rm SC}(0)$] of the 32-site supercells with rigid (ideal fcc) underlying lattice. Then the volume-relaxed vacancy formation energy was obtained as $H^N_{fu}(0) = E^N_{\rm SC}(0) - (N-1)E_0$, where N in our case is 32. Experiments show that the crystal structure is distorted around the vacancy. For a more realistic geometry around the vacancy, in the present study we included the local lattice relaxation by computing the total energy of the supercell [$E_{\rm SC}(\eta)$] as a function of the distance $d = (1+\eta)d_0$ between the vacancy and the 12 atomic sites from the first coordination shell around the vacancy. Here, d_0 is the ideal unrelaxed nearest-neighbor distance in the fcc lattice. The final vacancy formation energy (H_{fr}) and the equilibrium local relaxation (η_0) around the vacancy is obtained from the minimum of the formation energy $H^N_{fr}(\eta) = E^N_{\rm SC}(\eta) - (N-1)E_0$, viz. $H^N_{fr} = \min_\eta H^N_{fr}(\eta) = H^N_{fr}(\eta_0)$. This type of local relaxation within the present mean-field approximation may be questioned. On the other hand, our previous study on simple and transition metals[43] showed that the size of the local relaxation is quite similar in different metals. Therefore we assume that relaxing the position of the coherent potential around the vacancy represents a reasonable approximation for the true local relaxation within the alloy.

C. Numerical details

The EMTO basis set included s, p, d, and f orbitals for bulk and supercell calculations. The one-electron equations were solved within the scalar-relativistic approximation using the frozen-core approach. The latter approximation is needed in order to push the theoretical volume of fcc Fe-Cr-Ni alloy toward larger volumes[39] and by that give a more realistic description of the local magnetic moments. For each element and crystal lattice, the EMTO Green's function was calculated self-consistently for 16 complex energy points distributed exponentially on a semicircular contour, which included states within 1.0 Ry below the Fermi level. In the one-center expansion of the full charge density, we adopted an l cutoff of 10. All potential spheres were set at the corresponding Wigner-Seitz spheres. For the local lattice relaxation around the vacancy, we used both compressed ($\eta = -6, -4, -2\%$) and expanded ($\eta = 2\%$) nearest-neighbor distances. The minimum of $E_v(\eta)$ was obtained from a second-order polynomial fit. The k-space sampling was performed with a uniform k mesh within the Brillouin zone. The number of k points was established (see Ref. 43) so that the numerical error of the vacancy formation energy would be below 0.01 eV. All calculations were performed at 0 K, i.e., we neglected all thermal, including phonon and spin-fluctuation, effects. Previous theoretical study[43] showed that the electronic entropy term at 500 K gives

TABLE I. Theoretical results for bulk (b) and vacancy containing (32 site) supercell (SC) Fe-Cr-Ni alloys as a function of Cr and Ni concentrations (Fe balance). We present the equilibrium Wigner-Seitz radii (w in Bohr), bulk moduli (B in GPa).

Cr	Ni	w_b	B_b	w_{SC}	B_{SC}
12.0	8.0	2.662	156.3	2.657	152.6
12.0	14.0	2.662	159.7	2.656	153.2
12.0	20.0	2.661	162.7	2.658	156.2
15.0	13.0	2.663	161.6	2.658	155.1
15.0	17.0	2.663	163.7	2.658	157.2
17.5	12.0	2.663	163.7	2.661	156.4
18.0	8.0	2.662	162.0	2.658	154.9
18.0	20.0	2.664	168.0	2.658	161.3
21.0	13.0	2.664	167.8	2.659	161.0
21.0	17.0	2.664	169.7	2.659	162.8
24.0	8.0	2.664	168.8	2.659	159.67
24.0	14.0	2.665	171.3	2.660	163.7
24.0	20.0	2.665	174.3	2.660	167.2

an effect of 0.01 eV in the vacancy formation energy. Our final error bar, to reflect all approximations from above, was set to be 0.03 eV.[43] The present investigation covers ternary alloys containing 12–24 atomic (at.) % Cr and 8–20 at. % Ni (balance Fe).

III. RESULTS

A. Properties of bulk Fe-Cr-Ni

The first step in the *ab initio* modeling of the monovacancies in austenitic steels is to find the theoretical equilibrium Wigner-Seitz radius and bulk modulus of paramagnetic fcc Fe-Cr-Ni alloys. Our results are shown in Table I (third and fourth columns) as a function of Cr and Ni content. The equilibrium Wigner-Seitz radius varies with composition within the range of ± 0.002 Bohr around 2.663 Bohr, and the bulk modulus within the range of ± 9 GPa around 165.3 GPa. Previous theoretical calculation yielded 165 GPa for the bulk modulus of the base alloy corresponding to the AISI 304.[22,26] Furthermore, for the equilibrium Wigner-Seitz radius and bulk modulus of $Fe_{0.7}Ni_{0.15}Cr_{0.15}$, theory predicted 2.660 Bohr and 163 GPa, respectively,[48] compared to the experimental values of 2.65 Bohr and 159–162 GPa.[49] The present results from Table I are in perfect line with these former theoretical and experimental data.

The magnetic state of the fcc Fe-based paramagnetic alloys sensitively depends on the volume.[40] Therefore it is important that the used supercell has the right equilibrium lattice parameter (far away from the vacancy) in order to ensure a realistic (bulklike) environment for the vacancy. The theoretical equilibrium Wigner-Seitz radius and bulk modulus of the 32-site supercell containing one vacant site are listed in Table I (fifth and sixth columns). We observe that one vacancy per 32 sites has a minor effect on the average bulk parameters, meaning that the magnetic state of the alloy matrix is properly described by the present supercell.

B. Vacancy formation energies of homogeneous Fe-Cr-Ni alloys

The vacancy formation energies of pure elements vary with crystal structure and magnetic state. For Fe and Cr, there are no available experimental paramagnetic fcc monovacancy formation energies. For fcc Ni the recommended monovacancy formation enthalpy in fcc is 1.79 eV.[18]

The theoretical vacancy formation energies are listed in Table II. We find that the theoretical fully relaxed H_{fr} (volume-relaxed H_{fu}) increases from 1.83 to 2.04 eV (2.18 to 2.43 eV) as going from $Fe_{0.68}Ni_{0.20}Cr_{0.12}$ to $Fe_{0.72}Ni_{0.08}Cr_{0.20}$. Before discussing the obtained trends, we try to place these results on the palette of the existing experimental data for Fe-Cr-Ni. The volume relaxed formation energies are found to be larger than the recommended value (1.8 eV) for Fe-Cr-Ni alloys.[18] The difference between H_{fu} and H_{fr} gives the structural relaxation effect, which accounts for about 0.4 eV ($\sim$20%) for most concentrations. Our fully relaxed values fit well into 1.8–2.0 eV representing the range of experimental vacancy formation energies for austenitic Fe-Cr-Ni solid solution.[18] For commercial austenitic stainless-steel AISI316 the experimental vacancy formation enthalpy is 1.61 eV. This material usually contains 16−18% Cr, 10−14% Ni, and a few percent Si, Mn, and Mo, and max 0.08 wt. % C (balance Fe). For similar compositions, the present calculations give 1.90 eV. It was reported that the Si-vacancy interactions reduce the vacancy formation energy,[1–3,18] which may explain the difference between theory and experiment for the AISI316 alloy. Taking into account that the present study is based on the fully disordered model described within the mean-field approximation, we conclude that the agreement between the theoretical results from Table II and the available experimental data is satisfactory.

Since the vacancy formation energies of pure elements vary with crystal structure and magnetic state, it is rather difficult to discuss to what extent the rule of mixing for the vacancy formation energy works for Fe-Cr-Ni alloys. For fcc Ni, the recommended monovacancy formation enthalpy is 1.79 eV. However, for Fe and Cr, there are no available experimental paramagnetic fcc monovacancy formation energies. Thus in order to be able to see whether a linear interpolation between end members holds for the formation energy one should perform similar theoretical calculations for the hypothetical paramagnetic fcc Fe and Cr.

TABLE II. Theoretical results for vacancy formation energies in paramagnetic fcc Fe-Cr-Ni alloys as a function of Cr and Ni concentrations (Fe balance). We present the volume-relaxed (H_{fu}) and structure-relaxed (H_{fr}) vacancy formation energies (in eV).

Cr at.%		12			15		17.5	18		21			24	
Ni at. %	8	14	20	13	17	12	8	20	13	17	8	14	20	
H_{fu}	2.26	2.23	2.18	2.25	2.23	2.28	2.31	2.21	2.30	2.27	2.43	2.32	2.27	
H_{fr}	1.90	1.87	1.83	1.89	1.87	1.92	1.94	1.85	1.92	1.90	2.04	1.94	1.90	

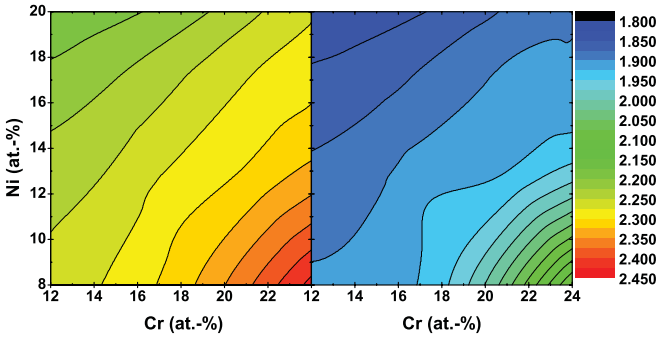

FIG. 1. (Color online) Vacancy formation energy (in units of eV) of homogeneous paramagnetic fcc Fe-Cr-Ni alloy as a function of chemical composition. Left panel: volume relaxed results; right panel: volume and structure relaxed results.

The volume-relaxed and volume plus structure-relaxed formation energies are plotted in Fig. 1 as a function of chemical composition. We notice that after structural relaxation the trend of the vacancy formation energies remains practically the same as that seen for the formation energies without local relaxation. This has been expected since by local relaxation we only change the size of vacancy but keep the mean-field environment almost constant. Figure 1 shows that the formation energy decreases (increases) monotonously with Ni (Cr). The effect of chemistry on the vacancy formation energies will be discussed in more detail in Sec. IV.

C. Vacancy effect on the local magnetic moments

Recent work investigated the effect of vacancy on the electronic Wigner-Seitz radius (charge density).[7] It was shown that the compensation effect in the charge density is not observable beyond the second nearest neighbor around the vacancy. Those observations turned our attention to verify the local magnetic moments in Fe-Cr-Ni alloys, where the magnetic state was found to have a large influence on the mechanical properties.[48] The paramagnetic state of Fe-Cr-Ni alloys was described within the disordered local magnetic-moment method. According to that, there are nonzero local magnetic moments on Fe atoms, but those on Cr and Ni atoms vanish (in lack of longitudinal spin fluctuations). The present results on the magnetic configuration of Fe-Cr-Ni supercells with vacancy are shown in Figs. 2–4.

We selected two series of Fe-Cr-Ni alloys in Fig. 2 to illustrate the compositional effect on the local magnetic moments. The open and filled symbols correspond to alloys with Cr content fixed to 24% and 12%, respectively, and with variable Ni content (8, 14, and 20%). In this way, one can follow how the moments vary with Cr and Ni content including the alloy with the lowest amount of Fe (encompassing 24% Cr and 20% Ni). In Fig. 2(a), the local magnetic moments are shown for all distinct nearest neighbors (coordination shells) within the 32-sites supercell. In order to compare the magnetic moments to the corresponding bulk values, in Fig. 2(b) we plot the shell-resolved moments for two alloys relative to their mean bulk values.

The variation of the local magnetic moments upon structural (local) relaxation around the vacancy are presented in Fig. 3 for the alloy containing 17.5% Cr and 12% Ni. Here, the vertical line marks the equilibrium local relaxation around the vacancy corresponding approximately to the vacancy formation energy minimum. Figure 4 displays the compositional map of the difference (δm in percent) between the average local magnetic moment in the supercell with vacancy and the corresponding bulk value. The difference is defined as $\delta m = (m_b - m_s)/m_b$, where m_b is the bulk local magnetic moment and m_s is the average supercell local magnetic moment. The trends from Figs. 2–4 will be discussed in Sec. IV.

IV. DISCUSSION

A. Trends of the vacancy formation energy

In the Landolt-Börnstein database for experimental results[18] there are two graphs for the vacancy formation energies. One is for 16 wt. % Cr and Ni content varying from

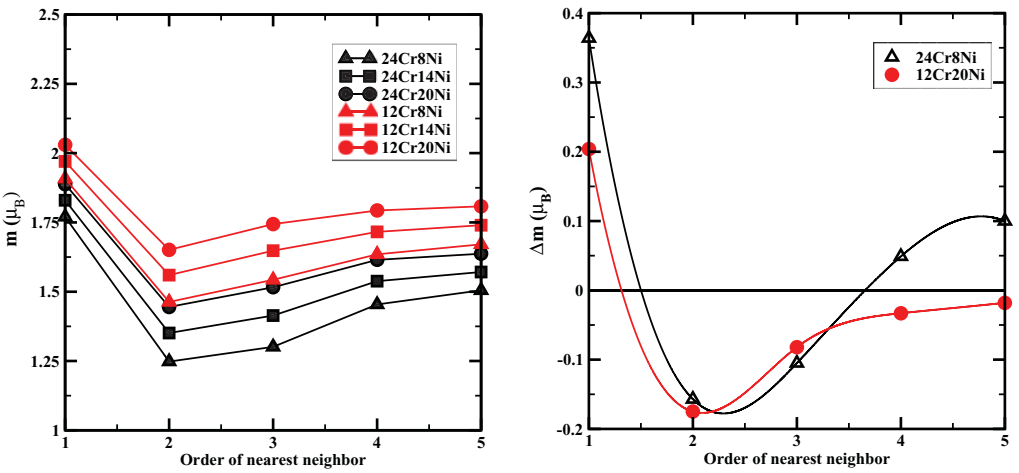

FIG. 2. (Color online) The chemical effect on the local magnetic moments (in μ_B) (panel a), and the deviation from the mean bulk magnetic moment for the two most extreme compositions (panel b). The local magnetic moments are shown as a function of the order of the nearest neighbor atomic sites (coordination shells).

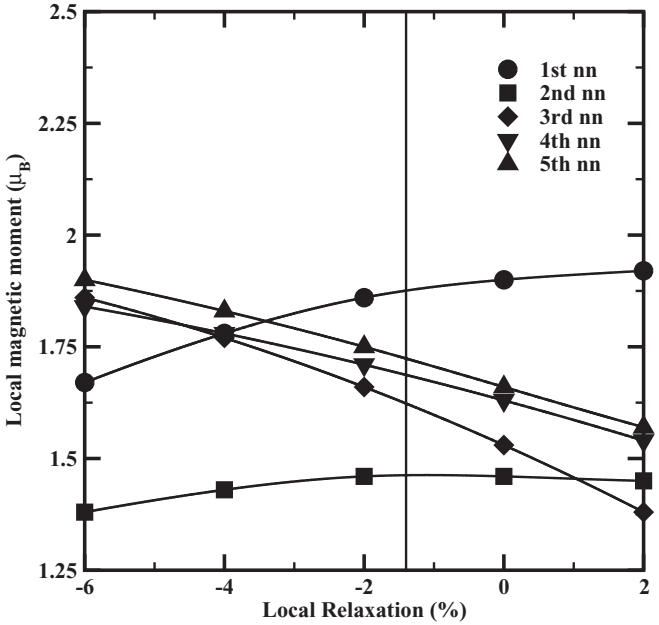

FIG. 3. Local magnetic moments (in μ_B) of the nearest-neighbor atoms around the vacant site as a function of local relaxation (η). The vertical line shows the equilibrium relaxation (η_0) corresponding to the minimum of $H_{fr}(\eta)$.

20 to 75 wt. %. For this system, the vacancy formation enthalpy scans values from 2.00 to 1.50 eV with increasing Ni content. In the second graph, the Ni content is fixed to 25 wt. % and the Cr content changes from 8 to 16 wt. %. In this case, the vacancy formation enthalpy scans values between 1.60 and 1.80 eV. For a compound with 25% Ni and 16% Cr we get 1.95 eV from the first and 1.80 eV on the second graph. However, both graphs contain large error bars which may explain this apparent inconsistency between them. It was also

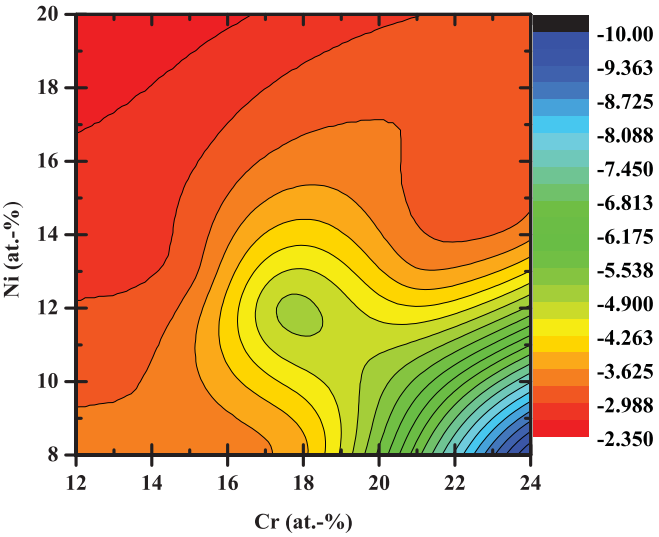

FIG. 4. (Color online) The difference (in percent) between the average local magnetic moment in the Fe-Cr-Ni supercell with vacancy and the corresponding bulk value plotted against the chemical composition.

mentioned that in pure Fe-Cr-Ni solid solution the vacancy formation energy depends on the short-range order in bulk alloy.

In experiments, the vacancy formation enthalpy is given by the difference of the self-diffusion coefficient and the vacancy migration enthalpy.[2,18] Checking the corresponding figures and tables from Ref. 18 we notice that neither the vacancy migration enthalpies nor the self-diffusion coefficient change with composition. Substracting these energies from each other will give an average 1.8 eV vacancy formation enthalpy (recommended value in Ref. 18). The reported weak compositional dependence could be the results of the annealing after the electron irradiation, which helps the relaxation of the crystal to reduce the effect of defects by recrystallization and diffusion. The above experimental values from Ref. 18 agree well with the results reported by Dimitrov and Dimitrov.[50] According to these authors, the vacancy formation energy is 2.02 and 1.84 eV, for Fe-Cr-Ni containing 20 and 45 wt. % Ni, respectively, and 16 wt. % Cr.

Our theoretical formation energies range from 1.83 to 2.04 eV as we go from Fe12Cr20Ni to Fe24Cr8Ni. These values are in line with the above experimental data.[18,50] The compositional dependence of the theoretical formation enthalpy shows the same trend as in experiments. Namely, increasing Ni content lowers the vacancy formation energy and increasing Cr content increases it. The small differences in the theoretical and experimental slopes can be attributed to the the differences in sample preparations and the approximations used in the theoretical description.

Quite interestingly, the compositional changes (segregation) in the nearest neighbor (nn) sites around the vacancy shows the same behavior as the one found in the experiments mentioned above and also in the present theoretical results. Here we quote a comprehensive test performed on Fe-Cr alloys done by del Rio *et al.*[5] and Olsson *et al.*[4] Despite the body-centered-cubic (bcc) structure used in these theoretical works, with decreasing the Cr content in the first nn the vacancy formation energy drops to the values found for the host bcc Fe. In our theoretical results, by reducing the Cr coordination around the vacancy, the vacancy formation energy decreases to the theoretical vacancy formation enthalpies found for fcc Ni and paramagnetic fcc Fe.[17,43]

B. Effective chemical potentials

To shed more light on the trends of the vacancy formation energy, we study the effective chemical potential (ECP) representing a measure of the interaction between alloy components and vacancy. Here we focus on the first coordination shell around the vacancy (first nearest neighbor) and on the fifth coordination shell, the latter corresponding approximately the bulk ECP. In these additional calculations, we consider a ternary alloy $Fe_{1-n-c}Ni_nCr_c$ containing 17.5% Cr ($c = 0.175$) and 12% Ni ($n = 0.12$). Numerically, the Cr-Fe effective chemical potential was computed according to

$$\Delta\mu^s_{\text{Cr-Fe}} \equiv \mu^s_{\text{Cr}} - \mu^s_{\text{Fe}} = \frac{\partial E^s_{\text{SC}}(n,c)}{\partial c} \approx \frac{E^s_{\text{SC}}(n,c+0.01) - E_{\text{SC}}(n,c)}{0.01}, \quad (1)$$

where $E_{SC}(n,c)$ is the total energy of the 32-site supercell with base composition on all atomic sites, $E^s_{SC}(n,c+0.01)$ is the total energy of the supercell with 1% concentration variation in the first ($s=1$) or fifth ($s=5$) coordination shell. A similar expression was used for the Ni-Fe ECP, $\Delta\mu^s_{Ni-Fe}$. We find that in case of Ni-Fe exchange process, the effective chemical potentials are $\Delta\mu^1_{Ni-Fe}=-35.042\,967$ Ry and $\Delta\mu^5_{Ni-Fe}=-35.041\,200$ Ry. For Cr, these figures change to $\Delta\mu^1_{Cr-Fe}=+23.445\,442$ Ry and $\Delta\mu^5_{Cr-Fe}=+23.443\,500$ Ry. Therefore, according to the theoretical effective chemical potentials, Ni atoms prefer positions near the vacancy (within the first coordination around the vacancy), whereas Cr atoms do not. This finding is in perfect agreement with the trends calculated for the vacancy formation energy.

The "segregation energy" around the vacancy in the case of Ni becomes $\Delta\mu^1_{Ni-Fe}-\Delta\mu^5_{Ni-Fe}=-1.767$ mRy/atom and that for Cr becomes $\Delta\mu^1_{Cr-Fe}-\Delta\mu^5_{Cr-Fe}=1.942$ mRy/atom. That is, it is slightly more likely to meet a Cr depleted zone near the vacancy than a Ni enriched zone. Assuming infinitely large bulk reservoir, at thermodynamic equilibrium the Ni (Cr) segregation (desegregation) should eventually lead to Ni-rich coordination around the vacancy. Since the ECPs are composition dependent (even at static conditions), the equilibrium concentration "profile" will realize when the difference between surface and bulk ECPs vanish (or when we reach a pure Ni coordination).

With increasing temperature, the configurational entropy opposes the Ni-Fe or Cr-Fe exchange process favoring a more homogenous distribution of the alloy components around the vacancy. We illustrate this effect by considering the Ni-Fe exchange in an alloy with homogeneous Cr content and neglecting the concentration dependence of the ECP. From the condition of vanishing $\Delta\mu^1_{Ni-Fe}(T)-\Delta\mu^5_{Ni-Fe}(T)\approx\Delta\mu^1_{Ni-Fe}-\Delta\mu^5_{Ni-Fe}+k_BT\ln\left[n^1(1-n-c)/n/(1-n^1-c)\right]$, at temperature T the equilibrium Ni concentration in the first coordination around the vacancy becomes

$$n^1=\frac{n(1-c)}{n+(1-c-n)e^{(\Delta\mu^1_{Ni-Fe}-\Delta\mu^5_{Ni-Fe})/(k_BT)}},\qquad(2)$$

where k_B is the Boltzmann constant. At $T=0$ K, we obtain $n^1=(1-c)$, i.e., all Fe atoms from the first coordination shell are changed to Ni. At $T=300$ K, $n^1=0.25$, i.e., at room temperature the Ni concentration around the vacancy is about double that of the bulk value. On the other hand, at 1000 K, we get $n^1=0.15$. This means that already at relatively low temperatures, the equilibrium concentration of Ni in the first nearest-neighbor sites is close to its bulk value. This result confirms the validity of our theoretical study performed on homogenous alloys. Furthermore, the above finding is in line with the earlier experimental conclusion,[2] namely that Cr moves away from the vacancies while Ni segregates to them.

C. Local magnetic moment variations

It was reported[16,51] that the nonlocal effect, that includes the variations of the charge and magnetic moments, accounts for about 0.6 eV in the vacancy formation energy of Ni and Fe. In order to reveal these effects in the vacancy formation energy of the Fe-Cr-Ni alloys, Fig. 2 displays the local magnetic-moment variations as a function of distance from the vacancy. We can see that the local moments in the fifth coordination shell still do not reach the bulk magnetization. This indicates that the effect of vacancy has a longer range on the local moments than on the charge density.[7] The role of chemistry on the local magnetic-moment wave is also visible in Fig. 2. Increasing Ni concentration raises the magnetic moments while increasing Cr concentrations lowers them. The slope of the magnetic wave changes when moving from high-Cr content to high-Ni content. This should be attributed to the different magnetic properties of the alloying elements. On the right-hand side of Fig. 2, we can see that Ni addition and Cr removal reduce the range of the falloff in the magnetic moment.

In Fig. 3, we plotted the local moments for the nearest-neighbor (nn) atoms as a function of local lattice relaxation around the vacancy (η). The $\eta=-6$ point depicts a fairly distorted system with minimum volume for the vacancy and maximized volume for the first nn atom. The opposite is the $\eta=+2$ point where the vacancy has the maximum volume. The first nn local moments increase with the volume of the vacancy, whereas the moments on the second nn remain almost constant. The third, fourth, and fifth nn moments, on the other hand, show a decreasing trend with increasing volume of the vacancy. The above variations are in line with the oscillatory behavior of the magnetic moments with increasing distance from the vacancy [Fig. 2(b)].

The difference between the bulk magnetic moment and the mean supercell magnetic moment (δm, Fig. 4) is always negative and shows a clear chemical composition dependence. We see higher deviations for the Cr rich alloys (up to -10%) and smaller deviations for the Ni rich alloys ($\lesssim-3\%$). Using *ab inito* alloy theory, Vitos and Johansson[48] demonstrated that the elastic properties of paramagnetic Fe-Cr-Ni alloys depend sensitively on the local magnetic moment. According to Fig. 4, the mean local magnetic moment increases around the vacancy, meaning that there is a magnetism-driven elastic softening around the vacancy. Using Fig. 1 from Ref. 48, we find that 10% increase in the average local magnetic moment results in about 10–20 K (2–4%) decrease of the elastic Debye temperature.

V. CONCLUSIONS

Using the exact muffin-tin orbitals method, we have calculated the equation of state and vacancy formation energies for paramagnetic fcc Fe-Cr-Ni alloys. All self-consistent calculations have been carried out within the local density approximation and using non-self-consistent generalized gradient approximation for the total energy. Using former theoretical data, we have concluded that the present theoretical approach with 0.03-eV error bar is suitable to calculate the formation energies of monovacancies in Fe-Cr-Ni ternary alloys.

We have demonstrated that structural relaxation has a major impact on vacancy formation energies. Our results show similar behavior as those found earlier by experiments and by the limited number of theoretical calculations. According to the predicted scenario, Cr increases and Ni decreases the vacancy formation energies. Segregation around the vacancy should eventually lead to Ni-rich coordination around the

vacancy at low temperatures, but this effect is strongly diminished at temperatures around 1000 K. In addition to the above chemical trends, volume effects are also found to have a marked effect on the formation energy. Our work calls for further theoretical investigations where the interactions between vacancy and alloy components are accounted for and the structural relaxations are treated beyond the present mean-field approach.

ACKNOWLEDGMENTS

The Swedish Research Council, the European Research Council, Swedish Steel Producer's Association, the Swedish Energy Agency and the Hungarian Scientific Research Fund (OTKA Project No. 84078) are acknowledged for financial support. Calculations were performed on NSC-Matter resources.

[1]G. M. Michal, F. Ernst, and A. H. Heuer, Metall. Mater. Trans. A **37**, 1824 (2006).
[2]S. J. Rothman, L. J. Nowicki, and G. E. Murch, J. Phys. F **10**, 383 (1980).
[3]B. Chakraborty, L. C. Smedskjaer, and S. J. Rothman, J. Phys. F **14**, 301 (1984).
[4]P. Olsson, C. Domain, and J. Wallenius, Phys. Rev. B **75**, 014110 (2007).
[5]E. del Rio, J. M. Sampedro, H. Dogo, M. J. Caturla, M. Caro, A. Caro, and J. M. Perlado, J. Nucl. Mater. **408**, 18 (2011).
[6]P. Hohenberg and W. Kohn, Phys. Rev. **136**, B864 (1964).
[7]L. Delczeg, E. K. Delczeg-Czirjak, B. Johansson, and L. Vitos, J. Phys.: Condens. Matter **23**, 045006 (2010).
[8]W. Kohn and L. J. Sham, Phys. Rev. **140**, A1133 (1965).
[9]J. P. Perdew, K. Burke, and M. Ernzerhof, Phys. Rev. Lett. **77**, 3865 (1996).
[10]R. Armiento and A. E. Mattsson, Phys. Rev. B **72**, 085108 (2005).
[11]N. Chetty, M. Weinert, T. S. Rahman, and J. W. Davenport, Phys. Rev. B **52**, 6313 (1995).
[12]D. E. Turner, Z. Z. Zhu, C. T. Chan, and K. M. Ho, Phys. Rev. B **55**, 13842 (1997).
[13]T. Hoshino, N. Papanikolaou, R. Zeller, P. H. Dederichs, M. Asato, T. Asada, and N. Stefanou, Comput. Mater. Sci. **14**, 56 (1999).
[14]K. M. Carling, G. Wahnström, T. R. Mattsson, A. E. Mattsson, N. Sandberg, and G. Grimvall, Phys. Rev. Lett. **85**, 3862 (2000).
[15]K. M. Carling, G. Wahnström, T. R. Mattsson, N. Sandberg, and G. Grimvall, Phys. Rev. B **67**, 054101 (2003).
[16]T. Mizuno, M. Asato, T. Hoshino, and K. Kawakami, J. Magn. Magn. Mater. **226–230**, 386 (2001).
[17]P. A. Korzhavyi, I. A. Abrikosov, B. Johansson, A. V. Ruban, and H. L. Skriver, Phys. Rev. B **59**, 11693 (1999).
[18]P. Ehrhart, P. Jung, H. Schultz, and H. Ullmaier, in *Atomic Defects in Metals*, edited by H. Ullmaier, Landolt-Börnstein, New Series, Group III, Vol. 25 (Springer-Verlag, Berlin, 1991), pp. 345–349.
[19]O. K. Andersen, O. Jepsen, and G. Krier, in *Lectures on Methods of Electronic Structure Calculation* (World Scientific, Singapore, 1994), p. 63.
[20]L. Vitos, H. L. Skriver, B. Johansson, and J. Kollár, Comput. Mater. Sci. **18**, 24 (2000).
[21]L. Vitos, Phys. Rev. B **64**, 014107 (2001).
[22]L. Vitos, in *Computational Quantum Mechanics for Materials Engineers* (Springer-Verlag, London, 2007), Chap. 9.
[23]B. L. Gyorffy, Phys. Rev. B **5**, 2382 (1972).
[24]M. Zwierzycki and O. K. Andersen, Acta Phys. Pol. A **115**, 64 (2009).
[25]J. Kollár, L. Vitos, and H. L. Skriver, in *Electronic Structure and Physical Properties of Solids: The Uses of the LMTO Method*, edited by H. Dreyssé, Lectures Notes in Physics (Springer-Verlag, Berlin, 2000), p. 85.
[26]L. Vitos, P. A. Korzhavyi, and B. Johansson, Phys. Rev. Lett. **88**, 155501 (2002); Nat. Mater. **2**, 25 (2003).
[27]P. Olsson, I. A. Abrikosov, L. Vitos, and J. Wallenius, J. Nucl. Mater. **321**, 84 (2003).
[28]L. Dubrovinsky *et al.*, Nature (London) **422**, 58 (2003).
[29]L. Vitos, P. A. Korzhavyi, and B. Johansson, Phys. Rev. Lett. **96**, 117210 (2006).
[30]N. Dubrovinskaia *et al.*, Phys. Rev. Lett. **95**, 245502 (2005).
[31]A. Taga, L. Vitos, B. Johansson, and G. Grimvall, Phys. Rev. B **71**, 014201 (2005).
[32]L. Huang, L. Vitos, S. K. Kwon, B. Johansson, and R. Ahuja, Phys. Rev. B **73**, 104203 (2006).
[33]J. Zander, R. Sandström, and L. Vitos, Comput. Mater. Sci. **41**, 86 (2007).
[34]A. E. Kissavos, S. I. Simak, P. Olsson, L. Vitos, and I. A. Abrikosov, Comput. Mater. Sci. **35**, 1 (2006).
[35]B. Magyari-Köpe, G. Grimvall, and L. Vitos, Phys. Rev. B **66**, 064210 (2002).
[36]B. Magyari-Köpe, L. Vitos, and G. Grimvall, Phys. Rev. B **70**, 052102 (2004).
[37]J. P. Perdew and Y. Wang, Phys. Rev. B **45**, 13244 (1992).
[38]D. M. Ceperley and B. J. Alder, Phys. Rev. Lett. **45**, 566 (1980).
[39]H. L. Zhang, N. Al-Zoubi, B. Johansson, and L. Vitos, J. Appl. Phys. **110**, 073707 (2011).
[40]H. Zhang, B. Johansson, and L. Vitos, Phys. Rev. B **84**, 140411(R) (2011).
[41]M. Asato, A. Settels, T. Hoshino, T. Asada, S. Blügel, R. Zeller, and P. H. Dederichs, Phys. Rev. B **60**, 5202 (1999).
[42]M. Ropo, K. Kokko, and L. Vitos, Phys. Rev. B **77**, 195445 (2008).
[43]L. Delczeg, E. K. Delczeg-Czirjak, B. Johansson, and L. Vitos, Phys. Rev. B **80**, 205121 (2009).
[44]T. Oguchi, K. Terakura, and N. Hamada, J. Phys. F **13**, 145 (1983).
[45]B. L. Györffy, A. J. Pindor, G. M. Stocks, J. Staunton, and H. Winter, J. Phys. F **15**, 1337 (1985).
[46]F. J. Pinski, J. Staunton, B. L. Györffy, D. D. Johnson, and G. M. Stocks, Phys. Rev. Lett. **56**, 2096 (1986).
[47]V. L. Moruzzi, J. F. Janak, and K. Schwarz, Phys. Rev. B **37**, 790 (1988).
[48]L. Vitos and B. Johansson, Phys. Rev. B **79**, 024415 (2009).
[49]A. Teklu, H. Ledbetter, S. Kim, L. A. Boatner, M. McGuire, and V. Keppens, Metall. Mater. Trans. A **35**, 3149 (2004).
[50]C. Dimitrov and O. Dimitrov, J. Phys. F **14**, 793 (1984).
[51]T. Hoshino, M. Asato, and T. Mizuno, J. Magn. Magn. Mater. **226–230**, 384 (2001).